

# Nanoscale

Accepted Manuscript



This is an *Accepted Manuscript*, which has been through the Royal Society of Chemistry peer review process and has been accepted for publication.

*Accepted Manuscripts* are published online shortly after acceptance, before technical editing, formatting and proof reading. Using this free service, authors can make their results available to the community, in citable form, before we publish the edited article. We will replace this *Accepted Manuscript* with the edited and formatted *Advance Article* as soon as it is available.

You can find more information about *Accepted Manuscripts* in the [Information for Authors](#).

Please note that technical editing may introduce minor changes to the text and/or graphics, which may alter content. The journal's standard [Terms & Conditions](#) and the [Ethical guidelines](#) still apply. In no event shall the Royal Society of Chemistry be held responsible for any errors or omissions in this *Accepted Manuscript* or any consequences arising from the use of any information it contains.

# Mesoscale Mechanics of Twisting Carbon Nanotube Yarns

Reza Mirzaeifar<sup>1,\*</sup>, Zhao Qin<sup>1</sup>, Markus J. Buehler<sup>1,†</sup>

<sup>1</sup> Laboratory for Atomistic and Molecular Mechanics, Department of Civil and Environmental Engineering, Massachusetts Institute of Technology, 77 Massachusetts Ave., Cambridge, MA, USA

<sup>†</sup> Corresponding author: E-mail: [mbuehler@MIT.EDU](mailto:mbuehler@MIT.EDU), phone: +1-617-452-2750, lab URL: <http://web.mit.edu/mbuehler/www/>

**Abstract:** Fabricating continuous macroscopic carbon nanotube (CNT) yarns with mechanical properties close to the individual CNTs remains a major challenge. Spinning CNT fibers and ribbons for enhancing the weak interactions between the nanotubes is a simple and efficient method for fabricating high-strength and tough continuous yarns. Here we investigate the mesoscale mechanics of twisting CNT yarns using full atomistic and coarse grained molecular dynamics simulations, considering concurrent mechanisms at multiple length-scales. To investigate the mechanical response of such a complex structure without losing insights into the molecular mechanism, we apply a multiscale strategy. The full atomistic results are used for training a coarse grained model for studying larger systems consisting several CNTs. The mesoscopic model parameters are updated as a function of twist angle, based on the full atomistic results, in order to incorporate the atomistic scale deformation mechanisms in the larger scale simulations. By bridging across two length scales, our model is capable of accurately predicting the mechanical behavior of twisted yarns while the atomistic level deformations in individual nanotubes are integrated into the model through updating the parameters. Our results focused on studying a bundle of closed packed nanotubes provides the novel mechanistic insights into the spinning of CNTs. Our simulations reveal how twisting a bundle of CNTs improves the shear interaction between the nanotubes up to a certain level due to increasing the interaction surface. Further twisting the bundle weakens the intertube interactions due to excessive deformations in the cross sections of individual CNTs in the bundle.

**Keywords:** Carbon Nanotube, Molecular Dynamics, Spinning, Mesoscale Model, Intertube Interaction

**Submitted to:** *Nanoscale*

## 1. Introduction

Carbon nanotubes (CNTs) have superior material properties including extremely high tensile stress, high modulus, high electrical and thermal conductivity and low density. However, despite the unique properties of individual CNTs, it remains a major challenge to fabricate macroscale structures made of CNTs which can fully retain the outstanding nanoscale properties of CNTs. Continuous CNT yarns are among the most attractive industrial structures to be made from individual CNTs. These yarns are

---

\* Present address: Mechanical Engineering Department, Virginia Polytechnic Institute and State University, Blacksburg, VA 24061, USA

fabricated from a large number of short tubes stacked together to create the macroscale structure. By this configuration, the strength of the macroscale yarn is governed by the intertube interactions, which are remarkably weaker compared to the strength of each CNT [1]. Despite many attempts in finding processes for maximizing the intertube interactions, there is still a challenge in developing a simple method for enhancing the weak interactions between the CNTs in a macroscale yarn and fabricating a fiber with mechanical properties even close to the superior properties of individual CNTs.

In recent years several approaches have been implemented to enhance the shear interaction between CNTs including chemical functionalization of CNTs [2-4], intertube bridging [5, 6], manufacturing spring-like carbon nanotube ropes [7], fabricating highly twisted double-helix CNT Yarns [8], fabricating tightly wound helical carbon nanotubes (HCNTs) [9], and wet or dry spinning CNT yarns [10-20]. Among these methods, spinning CNT yarns, either directly from as-grown super-aligned CNTs [13, 15, 18, 21, 22] or twisting CNT films [23, 24], has been the focus of much attention mainly because of its simplicity and capability of producing long continuous and neat fibers. Despite some successful attempts for fabricating strong spun yarns from CNTs, some experiments have shown that spinning may weaken the strength of fabricated yarns [12, 15, 16]. This reveals the necessity of more detailed fundamental investigations for better understanding the effect of twisting on the mechanical properties of CNT yarns. Some experimental studies have shown that there is an optimum twist angle for improving the strength and further spinning the yarn above this angle severely weakens the yarn [12, 16]. In order to better understand this phenomenon, here we implement a mesoscale numerical study to investigate the effect of twisting on the mechanical properties of CNT yarns at the atomistic level. Our molecular dynamics simulations provides the novel mechanistic insights into the effect of spinning CNTs at the atomistic level. The molecular dynamics simulations show how twisting a bundle of CNTs improves the shear interaction between the nanotubes up to a certain level, mainly due to increasing the interaction surface. It is also shown that the intertube interaction weaken by further twisting the bundle due to excessive deformation in the cross sections of individual CNTs in the bundle.

In addition to the full atomistic studies, we also have studied larger systems consisting of several CNTs by implementing a coarse grained (CG) model. In order to incorporate the atomistic scale deformation mechanisms, *i.e.*, the cross section changes in the individual tubes into the coarse grained model, we have introduced a novel strategy for bridging the two length scales by updating the coarse graining parameters based on the full atomistic results. Coarse grained models are powerful tools for studying the mechanical properties of CNT yarns, and these models have been recently used for studying the mechanical behavior and microstructural evolution of CNT continuous fibers under twisting and tension [25]. However, our results show that the mesoscale model should be trained by the atomistic results to bridge the gap between two different length scales. This strategy can be developed for studying various properties of CNTs by the coarse grained models more accurately. In studying large scaled CNT yarns we have considered two different conditions for investigating the properties of yarns fabricated by directly spinning as-grown super-aligned CNTs and also the yarns made by twisting CNT films. A recently developed strategy [26] is used in both cases for modeling the randomly entangled nanotubes in the forest or film of CNTs before the spinning.

## 2. Models and Methods

Both the full atomistic and coarse grained simulations are performed using the molecular dynamics package LAMMPS [27]. A full atomistic framework is used for calculating the changes in pull-out force of CNTs from twisted bundles in various conditions. These results are used for training a coarse grained model capable of studying CNT-based fibers composed of several nanotubes. By using the full atomistic results, the trained coarse grained model incorporates the smaller scale effects at the cross section of individual CNTs by updating the inter-tube van der Waals interactions as a function of twisting angle.

### 2.1. *Full atomistic simulation method*

For the full atomistic simulations, the CNTs are described by a Morse bond, a harmonic cosine bending angle, a twofold cosine torsion and a Lennard-Jones 12-6 interaction with the parameters given in [28]. This method of modeling CNTs has been successfully employed for studying self-assembly of single-walled CNTs into multiwalled CNTs in Water [28]. In order to study the accuracy of this method for analyzing the sliding of CNTs on each other, which is the major deformation mechanism in our simulations, we have considered some case studies including sliding two CNTs on each other, and the calculated shear forces obtained from this model are validated against similar test cases using the Adaptive Intermolecular Reactive Empirical Bond Order (AIREBO) potential [29]. A good agreement was observed in our results between the calculated shear force during sliding both single walled and double walled CNTs in all the case studies.

In order to better understand the nature of shear interaction between CNTs in twisted CNT yarns, full atomistic simulations are performed for calculating the force required to pull-out a CNT from the middle or outer layer of a closed packed bundle with seven CNTs. Full atomistic simulations are carried out under a microcanonical (NVT) ensemble (temperature control by a Berendsen thermostat [30]), with a time step of 0.1 fs. Two different cases are considered: (1) a seven-SWNT bundle with (5,5) nanotubes and (2) a bundle with seven (10,10)-(16,16) DWNTs. The length of each CNT in both bundles is 30 nm and the outer tubes are packed around a core tube. In order to study the effect of twisting on the pull-out force, the outer CNTs are twisted around the central axis by different angles. Instead of twisting the ends which causes high distortions near the clamped ends, a pure torsion is applied to all the atoms at the outer layer in which the twisting angle varies linearly through the length. Twisting is applied in several steps and at the end of each twisting increment the system is equilibrated by holding the ends to prevent the tubes from twisting back. It is worth noting that the total length selected in this paper (30 nm) is remarkably smaller than the typical length of CNT yarns. The selection of a small system is mainly due to the computational restrictions. However, the selected range of twisting angle per unit length in this paper matches the practical value which makes the results comparable at different length scales. As shown in this paper, the deformation mechanism in the cross section, which only depends on the twisting angle per length governs the mechanical response of intertube sliding. Also, we will use the coarse grained model besides the full atomistic simulations for studying relatively larger systems with lengths up to approximately 600 nm.

After twisting, the ends of all the tubes except the one which is pulled out are constrained and the system is equilibrated for another 20 ps. After equilibration, a pulling force is applied to one of the tubes using steered molecular dynamics (SMD), whereby the center of mass of the group of atoms at the end of pulled tube is connected by a harmonic spring to a dummy node which is moving with a constant speed in the axial direction. The strain rate effect is studied by applying the load at different rates and the rate of  $1\text{E} - 6\text{ fs}^{-1}$  is selected after making sure the convergence is achieved. The temperatures is set to  $T = 300\text{ K}$  in all the simulations.

## 2.2. Coarse-grained MD simulations method

The intertube interactions between CNTs in a closed pack bundle are studied using the full atomistic simulations. However, for studying larger yarns and fibers containing several nanotubes, the computational cost of full atomistic simulations is extremely high. We have used a mesoscopic bead-spring coarse grained model for studying the large yarns. This model has been proven to be a valid and efficient approach to simulate a variety of different configuration of CNT yarns and bundles [26, 31-33]. For obtaining the coarse grained parameters, a series of full atomistic mechanical tests are implemented. We focus on (10,10)-(16,16) DWNTs in the mesoscale simulations with the parameters previously reported as; equilibrium bead distance  $r_0 = 10\text{ nm}$ , tensile stiffness  $k_t = 2000\text{ kcal mol}^{-1}\text{\AA}^{-2}$ , equilibrium angle  $r_0 = 180^\circ$ , Bending stiffness  $k_\theta = 45000\text{ kcal mol}^{-1}\text{rad}^{-2}$ , and dispersive parameters  $\sigma = 22.63\text{ \AA}$ ,  $\varepsilon = 21.6\text{ kcal mol}^{-1}$ . For more details about extracting these parameters from a full atomistic model the reader is referred to [34]. The mentioned parameters have been implemented in a variety of mesoscale models and the accuracy of the constructed models is studied extensively in a series of previous works [26, 31-33].

## 3. Mechanics of twisting CNT yarns at the atomistic level

In order to study the effect of twisting on the mechanical response of CNT yarns, we start from studying this effect at the nanoscale, in which the tubes are modeled individually by a full atomistic representation. The results of the simulations at this scale reveal the deformation mechanism at the small scale, which are later used to train a coarse grained model capable of accurately studying the mechanical response of twisted CNT yarns at larger length scales. We consider the pull-out tests for both single walled and double walled closed packed bundles of CNTs in this section. Also, for having a more general representation we consider the cases of pulling out either the central or one of the side tubes from the closed packed bundle of seven nanotubes.

The force-displacement responses for different studied cases are shown in Figure 1 and 2. We have studied several twisting angles, while only four representative angles are shown in this figure for clarity. The reported angles in these figures are the average angle between each of the tubes at the outer layer and the axis of bundle, which is measured at the end of final equilibration before the pulling stage. The pull-out forces for the center and side tubes in a bundle of single walled CNTs are shown in Figure 1(a) and (b), respectively. It is observed that the maximum force for pulling out the central SWNT is slightly decreased at higher twist angles, while for the side tube the maximum force increases for the small twist angles ( $\theta < 10$ ) and then sharply decreases for the larger twist angles. It is worth noting that experimental values are not available for the pull-out of individual CNTs form a

closed packed bundle. However, the obtained force-displacement curves are consistent with the previously reported computational results on untwisted closed pack set of seven SWNTs [35], and a twisted bundle of SWNTs [36], although the results are not directly comparable because of the differences in the force fields and also the twisting methods. The comparison with the previously reported computational works will be further discussed in the following when we study the cross section deformations as well.

The overall trend is similar for DWNT bundles, as shown in Figure 2(a) and (s). The calculated maximum forces as functions of twist angles are shown in Figure 3 for both the single and double walled CNTs. The individual data points correspond to full atomistic simulations and the lines are polynomial curves fitted to the data points. As shown in Figure 3(a), the maximum pull-out force for the middle tube monotonically decreases at higher twist angles, and the slope increases sharply at large twist angles. The maximum pull-out force for the side tubes reaches an optimum at a specific twist angle for both the SWNT and DWNT bundles as shown in Figure 3(b), followed by a sharp decrease in the force by further increasing the twist angle above the optimum value. It is worth noting that the pull-out force which is governed by the weak intertube interactions is remarkable lower than the force required to break a nanotube of the same kind. The reported theoretically calculated and experimentally measured tensile strength of individual CNTs varies between 150 nN for (5,5) SWNTs [34] to a range of 400-1340 nN for multiwalled carbon nanotubes depending on their diameter [37].

Another important observation in the full atomistic results is the higher sensitivity of DWNTs to the twisting angle. Although the maximum pull-out force is remarkably higher in DWNT bundles, the force starts decreasing at relatively lower twisting angles compared to the SWNT bundles. This phenomenon will be further studied in the following by considering the cross section deformations in the bundles. It is worth noting that since the deformation mechanism in a large-scaled twisted yarn is mostly governed by CNT-CNT sliding similar to the studied side tubes pull-out, it is expected that the macroscopic response of a twisted yarn is directly related to mechanics of side tubes pull-out. The general trend in these results is in agreement with some previously reported experimental data, which report an optimum twisting angle for enhancing the yarns strength [12, 16], and can shed light into mechanics of large-scaled CNT yarns.

The changes of maximum pull-out force at different twisting angles can be further studied by analyzing the deformed shape of CNTs in the spun bundles as shown in Figure 4. The overall deformed shape of the closed pack bundle and also the cross section deformations (at a mid-length section) are shown in this figure for both the double walled (left) and single walled (right) nanotubes. As shown in Figure 4, twisting makes a distortion in the cross section which increases the contact area between the adjacent tubes. The deformation induced by the twisting, also causes a decrease in the tubes center lines distance. Both these effects lead to an improvement in the maximum shear force up to a certain point at which the cross sections collapse and the highly distorted tubes start kinking at different regions along the length. Further twisting the nanotube above this point weakens the shear strength and may even cause the individual CNTs to break. The calculated cross sections deformations are compatible to those reported by Qian *et al.* [36] despite some minor differences which are mainly caused by the difference in the selected force fields and also the twisting method. The bundle is spun

by holding and twisting the outer tubes in [36], while our smooth and linear twisting method corresponds to spinning a very long bundle of CNTs, which is more close to the realistic case in which the CNTs lengths are much larger than the cross section dimensions. The pull-out force of a middle tube from a bundle of SWNTs is also studied in [36], and a linear increase followed by a sudden drop is reported for the force by increasing the twist angle. Our results contain a more comprehensive study of the pull-out force for both SWNT and DWNT bundles, besides considering the pull-out for the tubes at the outer layer which dominates the deformation mechanism in large-scaled twisted yarns. In order to scale up the study to larger length scales, a coarse grained model can be trained to incorporate the cross section deformations with the method explained in the following section.

#### 4. Bridging across length scales to capture the twisting effect at larger scales

Coarse grained simulation approaches allow the investigation of mechanical properties of larger CNT yarns composed of several nanotubes, which is computationally impractical to be performed by full atomistic models. The coarse grain representation of CNTs is developed based on the full atomistic calculations and by performing a set of standard mechanical tests to describe the nanotube behavior [34]. The mechanical behavior of individual CNTs should be studied by the MD model in three loading cases including tensile test to determine the Young's modulus, bending to determine the bending stiffness, and an assembly of two CNTs to determine the adhesion energy between different nanotubes [26, 34]. The parameters in the mesoscopic bead-spring model are derived by using the principal of energy conservation between full atomistic and coarse grained potentials.

The total energy of the system in the mesoscale model is expressed as

$$E = E_T + E_B + E_{pairs} = \sum_{bonds} \phi_t(r) + \sum_{angles} \phi_\theta(\theta) + \sum_{pairs} \phi_{ij}(r) \quad (1)$$

where  $E_T$  is the energy stored in the chemical bonds due to stretching along the axial direction,  $E_B$  is the energy due to bending of the CNT, and  $E_{pairs}$  constitutes the energy of vdW interactions. The total energy contribution of each part is given by the sum over all pair-wise and angular interactions in the system as expressed in the right hand side of Equation (1). For the axial stretching and bending stiffness, simple harmonic and rotational harmonic springs are considered respectively, to determine the energy between all bonded pairs and all triples of particles in the system as

$$\phi_t(r) = \frac{1}{2} k_t (r - r_0)^2, \quad \phi_\theta(\theta) = \frac{1}{2} k_\theta (\theta - \theta_0)^2 \quad (2)$$

where  $k_t$  is the spring constant relating distance  $r$  between two particles relative to the equilibrium distance  $r_0$  and  $k_\theta$  is the spring constant relating bending angle  $\theta$  between three particles relative to the equilibrium angle  $\theta_0 = 180^\circ$ . For obtaining the axial stiffness in the coarse grained model, the effective Young's modulus is directly calculated via force–displacement results from the full atomistic simulation and this effective Young's modulus is used for finding the equivalent  $k_t$  which results into the same strain energy in both the atomistic and coarse grained models in small deformations. In a

similar calculations, the bending stiffness  $EI$  is used from the full atomistic simulations to allow the formulation of elastic energy and an equivalent  $k_\theta$ . The major part of the energy which is affected by the twisting of CNTs and the changes that we have observed in the cross section is the  $E_{pairs}$  which corresponds to the vdW interactions. Also, as mentioned in the previous section, the strength of the macroscale yarn is governed by the intertube interactions which directly related to the vdW interactions.

We assume weak, dispersive interactions between either different parts of each molecule or different molecules (small segments of a CNT in this paper), defined by a Lennard–Jones 12:6 (LJ) function

$$\phi_{ij}(r) = 4\varepsilon \left[ \left( \frac{\sigma}{r} \right)^{12} - \left( \frac{\sigma}{r} \right)^6 \right] \quad (3)$$

where the  $ij$  parameters  $\sigma$  and  $\varepsilon$  are the distance parameter and the energy well depth at the equilibrium, respectively. These parameters can be calculated from the full atomistic model by equilibrating a system of two macromolecules to find the distance parameter, and measuring the change of energy by moving two equilibrated macromolecules apart to a large distance for calculating the energy well depth. The developed coarse grained model is incapable of incorporating the deformation mechanisms at the atomistic level, i.e. the cross section changes that were studied in the previous section. We will introduce a modification at the coarse grained model to bridge across the two length scales and capture the twisting effect at the larger scale.

It was shown in the previous section that the atomistic scale deformations have a significant effect on the mechanical response of CNTs sliding. The cross section deformations, as shown in Figure 4, play a significant role on the mechanical response of CNT yarns. These cross section deformations also effect the coarse grained parameters  $c$ ,  $k_\theta$ ,  $\sigma$  and  $\varepsilon$ . Among these, the distance parameter  $\sigma$  and the energy well depth  $\varepsilon$  has the most significant effect on the deformation mechanism of CNTs sliding on each other. In order to update these parameters as a function of twisting angle, the following training set is studied and the coarse grained parameters are updated based on the full atomistic results.

A set of seven closed pack DWNTs is modeled by the coarse grained model as shown in Figure 5(a), with the details explained in Section 2.2. The bundle is then subjected to a twisting with the same method as the full atomistic model is loaded. However, at each twisting angle, the inter-tube van der Waals interactions are updated by using the full atomistic simulation results. The dispersive distance is updated by calculating the average center to center distance between the tubes in the full atomistic bundle simulation, and the dispersive energy is updated by matching the force between the coarse grained and full atomistic model. A sample of matched force-displacement responses for two different twisting angles is shown in Figure 5(b). It is worth noting that since the changes in the sliding force at different twisting angles are originated from the deformation mechanisms at the atomistic level, if the vdW parameters are not updated in the coarse grained model, the predicted force deflection response in the coarse grained model is not affected significantly by applying the twisting on the bundle. The required vdW parameters for achieving the best match between the coarse grained and full atomistic models are calculated for a range of twisting angles as shown in Figure 5(c). These parameters can be

used for accurately studying the mechanical properties of large twisted CNT yarns, as explained with more details in the following section.

### 5. Updated coarse-grained model for twisted CNT yarns

Several attempts have been reported in the literature for developing coarse grained models for simulating the mechanical response of CNT yarns and bundles [25, 31, 33]. Here we use a unique approach which is inspired by the experimental observations in order to accurately study the deformation mechanics in twisted yarns. A method successfully used for studying the mechanical response of crosslinked CNT bundles is creating the bundle geometry by arranging the CNTs in a planar sheet and using a time dependent radial pressure to squeeze the nanotubes and constructing the bundle model [31]. The method has been successfully applied to study the effect of polymer crosslinking on the mechanical response of CNT bundles [31]. However, the twisting effect cannot be studied by this method. Also, the majority of individual nanotubes are parallel to each other at the modeled bundle. SEM images have clearly shown that the nanotubes are highly entangled in the twisted yarns. This entanglement has also been observed in CNT sheets or films (known as buckypapers).

A novel assembly procedure based on the coarse grain model of CNTs has been reported to attain an accurate representative mesoscopic buckypaper model that incorporates the entanglement in the CNTs forming the films at different layers [26]. Here we use a similar approach and construct a mesoscopic film composed of five CNT layers with random orientations wobbled within  $30^\circ$  around the axis. The five layers are assembled through a stepwise deposition in which the system is equilibrated for 10 ps after each layer is deposited on the substrate. In order to incorporate the randomness in the distribution of CNT lengths in the yarn, each layer consists 40 tubes with random lengths. The system is then subjected to a lateral pressure directed toward the substrate to model the vacuum filtration pressure. In order to model the CNTs entanglement, coarse grained parameters are manipulated during the assembly with a similar method used in [26]. In this method, bending stiffness and tube interaction parameters are reduced significantly during the assembly process. The reduced parameters are returned to the initial values in a final step, and the system is equilibrated and relaxed for 1 ns. A schematic of the equilibrated film is shown in Figure 6(a). This initial system is then used for constructing two different yarns as shown in Figure 6(b). The untwisted yarn is modeled by applying a cylindrical indentation to the equilibrated film as schematically shown in Figure 6(b). For modeling the twisted yarn, a linear twisting is applied to the equilibrated mat, similar to the twisting applied to the full atomist models in the previous sections. In this method, the whole simulation box is twisted around the axis which applies a varying twist angle to the system. We also have modeled some twisted yarns by holding the two ends and twisting the ends, but it was observed that the linear twisting method results into a smoother and more realistic final shape compared to twisting only the ends. Also, applying a linear twisting can be considered as modeling a very large yarn which is twisted at the ends and our model corresponds to the twisted areas far from the ends. The twisting is applied in a stepwise procedure and the system is equilibrated and relaxed after applying each increment of twisting. The final shape of a twisted and untwisted yarns are also shown in Figure 6(b).

Both the twisted and untwisted yarns are subjected to a tensile load to study the effect of twisting on the strength of yarns. As mentioned in the previous section, the vdW parameters in the coarse grained model are updated in the twisted yarn. It is worth noting that the angle of twist is not uniform in all the tubes in a yarn, particularly with the current model which also incorporates the entanglement, and we have approximately calculated a twisting angle by averaging the angle in different layers of the yarn. The end beads of the yarn, in a region within approximately 10 nm from each end, are fixed rigid and the simulation box is stretched along the axis with a constant strain rate of  $0.1 \text{ ns}^{-1}$ . During the box stretching, the fixed ends are clamped to the box which simulates a displacement controlled straining of the yarn. In a finite-length yarn, the constituent nanotubes are remarkably shorter than the yarn length. As a result, the dominant deformation mechanism is the inter-tube shearing. In order to investigate this effect, a gap is introduced in each of the nanotubes at random locations between the fixed ends. The gaps are created by deleting the bonds, angles, and pair-wise interactions of two connecting beads in each nanotube. The energy contributions of deleted beads are also removed by excluding them from thermostat calculations [31]. In order to study the effect of twisting on the strength, the virial stress is calculated in a representative volume which does not include the fixed end and also the beads in the gaps. The virial stress is an equivalent definitions of the continuum stress at the atomic level calculated using the balance equations which is averaged over a volume and over a small time interval to reduce random and temperature-related stress fluctuations [38, 39]. Also, we use the term engineering strain as an equivalent of the strain in a continuum system and define that as  $\delta / L$ , where  $\delta$  is the total elongation of the yarn and  $L$  represents the initial length.

The stress versus engineering strain for a twisted and untwisted yarn is compared in Figure 7(a). In this case study the average angle of nanotubes in the twisted yarn is selected to match the angle which corresponds to the maximum pull-out force for DWNT bundles as shown in Figure 3 ( $\theta \sim 12$ ). It is worth noting that the twist angle in the CG model for yarns is different for each nanotube. In this paper, for qualitative studies we are assuming an average value in the yarn, but an extension of this work would be developing a CG model that calculates the twisting angles locally at each bead and then assigns appropriate  $lj$  parameters to that specific bead. For comparison purposes the stress-strain response predicted by the original coarse grained model is also shown in this figure. It is observed that when the vdW interactions are not updated in the coarse grained model, the simulation predicts a remarkable decrease in the strength by twisting the yarns, which is erroneous since this model is not considering the geometrical deformations at the atomistic level, as explained in the previous section. In the original coarse grained model, twisting the yarn increases the distance between beads in adjacent tubes which consequently causes a decrease in the strength. However, the updated coarse grained model, which incorporates the smaller scale deformations by updating the vdW interactions, shows the improvement caused by twisting on both the strength and toughness of the yarn consistent with the experimental results [19]. The stress-strain responses exhibit a sharp initial slope, which is remarkably higher for the twisted yarn. This sharp initial response corresponds to the case that the applied force, which is monotonically increasing, is not sufficient to overcome the vdW interaction between the tubes and the displacements are negligible. The value of force at which sliding begins is larger for the twisted yarns, mainly because the vdW interactions are stronger. The deformation of both untwisted and twisted yarns subjected to axial tension are also shown in Figure 7(b) and (c), respectively. The developed framework can be used as an efficient tool for finding the optimum twisting angle for CNT

yarns with various configurations, particularly to find the optimum combination of applied axial force and twisting rate in fabricating long spun yarns. As another case study, in the next section we study a larger yarn fabricated by spinning long ribbons of CNT mats.

An efficient method for creating high strength macroscopic CNT yarns is fabricating them by twisting narrow and long ribbons of CNT mats [23, 24, 40, 41]. The as-produced CNT mats are extremely porous which makes them very weak. Shrinking the yarns remarkably improves the mechanical properties of these mats by decreasing the porosity and enhancing the intertube interactions in the yarn. Here we study the mechanical properties of twisted CNT yarns fabricated by spinning nanotube mats followed by shrinking the yarn. Constructing the model is similar to the previous case study, with the difference that each layer contains several short nanotubes aligned with a random direction with respect to the axis as shown in Figure 8(a). The length of each nanotube is random but in the range of 5 to 10% the total length of the mat, which is set to approximately 600 nm. The nanotubes lengths are generated by a uniform pseudorandom function. Similar to the previous case, five layers of randomly aligned nanotubes are assembled on top of each other through a stepwise deposition and the system is equilibrated for 10 ps after each layer is deposited. In this case each layer contains a different number of CNTs (~600) with random lengths. The system is subjected to a lateral pressure after the deposition is completed. The entanglement of the CNTs is obtained in the model by the same strategy used in the previous case study. The equilibrated model shown in Figure 8(a) is used for constructing two different yarns from the mat as shown in Figure 8. The untwisted yarn which is modeled by applying a cylindrical indentation to the equilibrated mat and the twisted yarn are shown in Figure 8(b) and (c), respectively. Mechanical properties of these yarns are then investigated by applying a uniaxial tension on the yarn with the method explained in the previous sections. The stress-strain responses of the yarns are shown in Figure 9(a). It is clearly shown that both the strength and ductility are strongly improved by spinning the mat. The observed improvement is in agreement with the experimental measurements on larger spun CNT fibers [19]. For comparison purposes the stress-strain curve for the spun fiber without updating the coarse-grained parameters is also shown in Figure 9(a). Comparing the simulation results with the experimental measurements (i.e. Figure 3 in [19]), clearly shows that the model without updated coarse grained parameters is not able to simulate the mechanical response accurately. The deformation mechanisms for the non-twisted and twisted yarns are shown in Figure 9(b) and (c), respectively.

## 6. Conclusion

In this paper we introduced a mesoscale model applied to studying the mechanics of twisting carbon nanotube (CNT) yarns and fibers, and the effect of spinning on the mechanical response of the yarns. Full atomistic studies on small systems of closed packed single and double walled CNTs are performed for analyzing the deformation mechanics of nanotubes during twisting. Our results show that twisting the bundle enhances the intertube interactions in a bundle of CNTs up to a certain level by increasing the interaction area. By twisting the tubes more than the optimum angle, the excessive cross section deformations become prominent and weakens the intertube shear strength. A coarse grained model is developed by training the mesoscopic parameters based on the full atomistic model. The obtained coarse grained model bridges two different length scales and incorporates the CNTs deformations at

the atomistic level into the larger scale model, which facilitates accurately studying the mechanical behavior of twisted yarns with several CNTs.

## 7. Acknowledgements

The authors gratefully acknowledge the support from ARO through a MURI award, No. W911NF-09-1-0541. Additional support provided by AFOSR and DOD-PECASE.

## 8. REFERENCES

1. Nair, A.K., Qin Z., and Buehler M.J., *Cooperative deformation of carboxyl groups in functionalized carbon nanotubes*. International Journal of Solids and Structures, 2012. **49**(18): p. 2418-2423.
2. Naraghi, M., Bratzel G.H., Filleter T., An Z., Wei X.D., Nguyen S.T., Buehler M.J., and Espinosa H.D., *Atomistic investigation of load transfer between dwnt bundles "crosslinked" by pmma oligomers*. Advanced Functional Materials, 2013. **23**(15): p. 1883-1892.
3. Peng, B., Locascio M., Zapol P., Li S.Y., Mielke S.L., Schatz G.C., and Espinosa H.D., *Measurements of near-ultimate strength for multiwalled carbon nanotubes and irradiation-induced crosslinking improvements*. Nature Nanotechnology, 2008. **3**(10): p. 626-631.
4. Sahoo, N.G., Cheng H.K.F., Cai J.W., Li L., Chan S.H., Zhao J.H., and Yu S.Z., *Improvement of mechanical and thermal properties of carbon nanotube composites through nanotube functionalization and processing methods*. Materials Chemistry and Physics, 2009. **117**(1): p. 313-320.
5. Kis, A., Csanyi G., Salvétat J.P., Lee T.N., Couteau E., Kulik A.J., Benoit W., Brugger J., and Forro L., *Reinforcement of single-walled carbon nanotube bundles by intertube bridging*. Nature Materials, 2004. **3**(3): p. 153-157.
6. Filleter, T., Bernal R., Li S., and Espinosa H.D., *Ultrahigh strength and stiffness in cross-linked hierarchical carbon nanotube bundles*. Advanced Materials, 2011. **23**(25): p. 2855-2860.
7. Shang, Y., He X., Li Y., Zhang L., Li Z., Ji C., Shi E., Li P., Zhu K., and Peng Q., *Super-stretchable spring-like carbon nanotube ropes*. Advanced Materials, 2012. **24**(21): p. 2896-2900.
8. Shang, Y., Li Y., He X., Du S., Zhang L., Shi E., Wu S., Li Z., Li P., and Wei J., *Highly twisted double-helix carbon nanotube yarns*. Acs Nano, 2013. **7**(2): p. 1446-1453.
9. Wu, J., He J., Odegard G.M., Nagao S., Zheng Q., and Zhang Z., *Giant stretchability and reversibility of tightly wound helical carbon nanotubes*. Journal of the American Chemical Society, 2013. **135**(37): p. 13775-13785.
10. Cheng, T.-W. and Hsu W.-K., *Winding of single-walled carbon nanotube ropes: An effective load transfer*. Applied Physics Letters, 2007. **90**(12): p. 123102.
11. Ericson, L.M., Fan H., Peng H., Davis V.A., Zhou W., Sulpizio J., Wang Y., Booker R., Vavro J., and Guthy C., *Macroscopic, neat, single-walled carbon nanotube fibers*. Science, 2004. **305**(5689): p. 1447-1450.
12. Fang, S., Zhang M., Zakhidov A.A., and Baughman R.H., *Structure and process-dependent properties of solid-state spun carbon nanotube yarns*. Journal of Physics: Condensed Matter, 2010. **22**(33): p. 334221.
13. Jiang, K., Li Q., and Fan S., *Nanotechnology: Spinning continuous carbon nanotube yarns*. Nature, 2002. **419**(6909): p. 801-801.
14. Li, Y.-L., Kinloch I.A., and Windle A.H., *Direct spinning of carbon nanotube fibers from chemical vapor deposition synthesis*. Science, 2004. **304**(5668): p. 276-278.

15. Liu, K., Sun Y., Zhou R., Zhu H., Wang J., Liu L., Fan S., and Jiang K., *Carbon nanotube yarns with high tensile strength made by a twisting and shrinking method*. Nanotechnology, 2010. **21**(4): p. 045708.
16. Miao, M., McDonnell J., Vuckovic L., and Hawkins S.C., *Poisson's ratio and porosity of carbon nanotube dry-spun yarns*. Carbon, 2010. **48**(10): p. 2802-2811.
17. Tran, C.D., Humphries W., Smith S.M., Huynh C., and Lucas S., *Improving the tensile strength of carbon nanotube spun yarns using a modified spinning process*. Carbon, 2009. **47**(11): p. 2662-2670.
18. Zhang, M., Atkinson K.R., and Baughman R.H., *Multifunctional carbon nanotube yarns by downsizing an ancient technology*. Science, 2004. **306**(5700): p. 1358-1361.
19. Zhang, X., Li Q., Tu Y., Li Y., Coulter J.Y., Zheng L., Zhao Y., Jia Q., Peterson D.E., and Zhu Y., *Strong carbon nanotube fibers spun from long carbon nanotube arrays*. Small, 2007. **3**(2): p. 244-248.
20. Lima, M.D., Li N., De Andrade M.J., Fang S., Oh J., Spinks G.M., Kozlov M.E., Haines C.S., Suh D., and Foroughi J., *Electrically, chemically, and photonically powered torsional and tensile actuation of hybrid carbon nanotube yarn muscles*. Science, 2012. **338**(6109): p. 928-932.
21. Zhang, X.B., Jiang K.L., Teng C., Liu P., Zhang L., Kong J., Zhang T.H., Li Q.Q., and Fan S.S., *Spinning and processing continuous yarns from 4-inch wafer scale super-aligned carbon nanotube arrays*. Advanced Materials, 2006. **18**(12): p. 1505-1510.
22. Zhang, X., Li Q., Holesinger T.G., Arendt P.N., Huang J., Kirven P.D., Clapp T.G., DePaula R.F., Liao X., Zhao Y., Zheng L., Peterson D.E., and Zhu Y., *Ultrastrong, stiff, and lightweight carbon-nanotube fibers*. Advanced Materials, 2007. **19**(23): p. 4198-4201.
23. Ma, W.J., Liu L.Q., Yang R., Zhang T.H., Zhang Z., Song L., Ren Y., Shen J., Niu Z.Q., Zhou W.Y., and Xie S.S., *Monitoring a micromechanical process in macroscale carbon nanotube films and fibers*. Advanced Materials, 2009. **21**(5): p. 603-608.
24. Ma, W.J., Liu L.Q., Zhang Z., Yang R., Liu G., Zhang T.H., An X.F., Yi X.S., Ren Y., Niu Z.Q., Li J.Z., Dong H.B., Zhou W.Y., Ajayan P.M., and Xie S.S., *High-strength composite fibers: Realizing true potential of carbon nanotubes in polymer matrix through continuous reticulate architecture and molecular level couplings*. Nano Letters, 2009. **9**(8): p. 2855-2861.
25. Liu, X., Lu W., Ayala O.M., Wang L.-P., Karlsson A.M., Yang Q., and Chou T.-W., *Microstructural evolution of carbon nanotube fibers: Deformation and strength mechanism*. Nanoscale, 2013. **5**(5): p. 2002-2008.
26. Cranford, S.W. and Buehler M.J., *In silico assembly and nanomechanical characterization of carbon nanotube buckypaper*. Nanotechnology, 2010. **21**(26): p. 265706.
27. Plimpton, S., *Fast parallel algorithms for short-range molecular-dynamics*. Journal of Computational Physics, 1995. **117**(1): p. 1-19.
28. Zou, J., Ji B., Feng X.-Q., and Gao H., *Self-assembly of single-walled carbon nanotubes into multiwalled carbon nanotubes in water: Molecular dynamics simulations*. Nano Letters, 2006. **6**(3): p. 430-434.
29. Stuart, S.J., Tutein A.B., and Harrison J.A., *A reactive potential for hydrocarbons with intermolecular interactions*. The Journal of Chemical Physics, 2000. **112**(14): p. 6472-6486.
30. Berendsen, H.J.C., Postma J.P.M., Vangunsteren W.F., Dinola A., and Haak J.R., *Molecular-dynamics with coupling to an external bath*. Journal of Chemical Physics, 1984. **81**(8): p. 3684-3690.
31. Bratzel, G.H., Cranford S.W., Espinosa H., and Buehler M.J., *Bioinspired noncovalently crosslinked "fuzzy" carbon nanotube bundles with superior toughness and strength*. Journal of Materials Chemistry, 2010. **20**(46): p. 10465-10474.

32. Cranford, S., Yao H., Ortiz C., and Buehler M.J., *A single degree of freedom 'lollipop' model for carbon nanotube bundle formation*. Journal of the Mechanics and Physics of Solids, 2010. **58**(3): p. 409-427.
33. Naraghi, M., Bratzel G.H., Filleter T., An Z., Wei X., Nguyen S.T., Buehler M.J., and Espinosa H.D., *Atomistic investigation of load transfer between dwnt bundles "crosslinked" by pmma oligomers*. Advanced Functional Materials, 2013. **23**(15): p. 1883-1892.
34. Buehler, M.J., *Mesoscale modeling of mechanics of carbon nanotubes: Self-assembly, self-folding, and fracture*. Journal of Materials Research, 2006. **21**(11): p. 2855-2869.
35. Filleter, T., Yockel S., Naraghi M., Paci J.T., Compton O.C., Mayes M.L., Nguyen S.T., Schatz G.C., and Espinosa H.D., *Experimental-computational study of shear interactions within double-walled carbon nanotube bundles*. Nano Letters, 2012. **12**(2): p. 732-742.
36. Qian, D., Wagner G.J., Liu W.K., Yu M.-F., and Ruoff R.S., *Mechanics of carbon nanotubes*. Applied Mechanics Reviews, 2002. **55**(6): p. 495-533.
37. Yu, M.-F., Lourie O., Dyer M.J., Moloni K., Kelly T.F., and Ruoff R.S., *Strength and breaking mechanism of multiwalled carbon nanotubes under tensile load*. Science, 2000. **287**(5453): p. 637-640.
38. Subramaniyan, A.K. and Sun C., *Continuum interpretation of virial stress in molecular simulations*. International Journal of Solids and Structures, 2008. **45**(14): p. 4340-4346.
39. Tsai, D., *The virial theorem and stress calculation in molecular dynamics*. The Journal of Chemical Physics, 1979. **70**(3): p. 1375-1382.
40. Beese, A.M., Sarkar S., Nair A., Naraghi M., An Z., Moravsky A., Loutfy R.O., Buehler M.J., Nguyen S.T., and Espinosa H.D., *Bio-inspired carbon nanotube-polymer composite yarns with hydrogen bond-mediated lateral interactions*. ACS Nano, 2013. **7**(4): p. 3434-3446.
41. Naraghi, M., Filleter T., Moravsky A., Locascio M., Loutfy R.O., and Espinosa H.D., *A multiscale study of high performance double-walled nanotube-polymer fibers*. ACS Nano, 2010. **4**(11): p. 6463-6476.

## Figures and Figure Captions

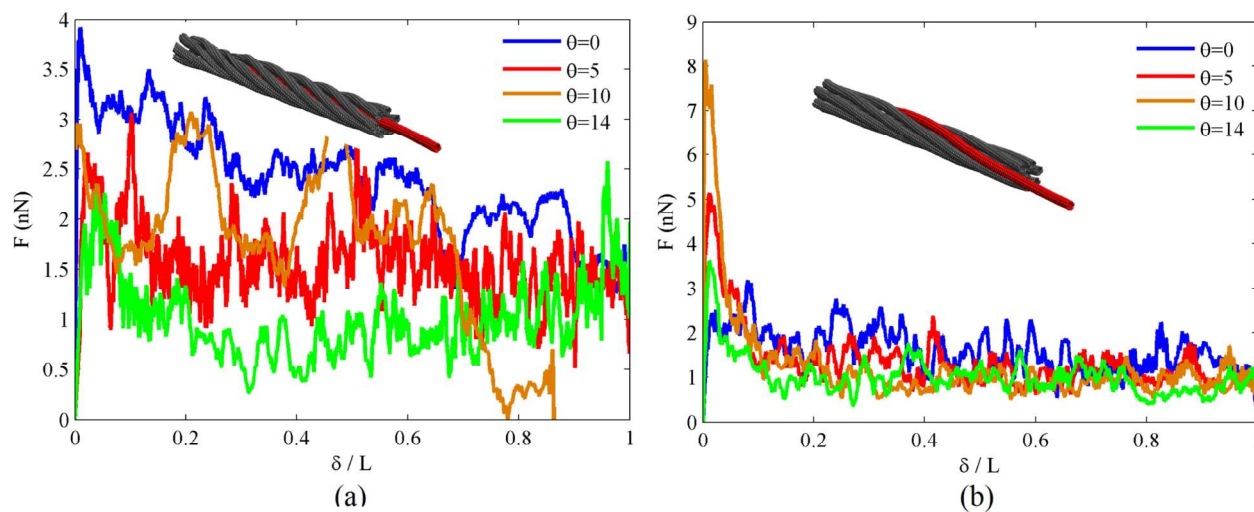


Figure 1: Pull-out forces for the (a) center and (b) side tubes in a bundle of single walled CNTs for four representative angles. Insets show the bundle and the pulled out nanotube is colored in red. The maximum force for pulling out the central nanotube is slightly decreased at higher twist angles, while for the side tube the maximum force increases for the small twist angles and then sharply decreases for the larger twist angles. The maximum pull-out force as a function of twist angle is further studied in Figure 3.

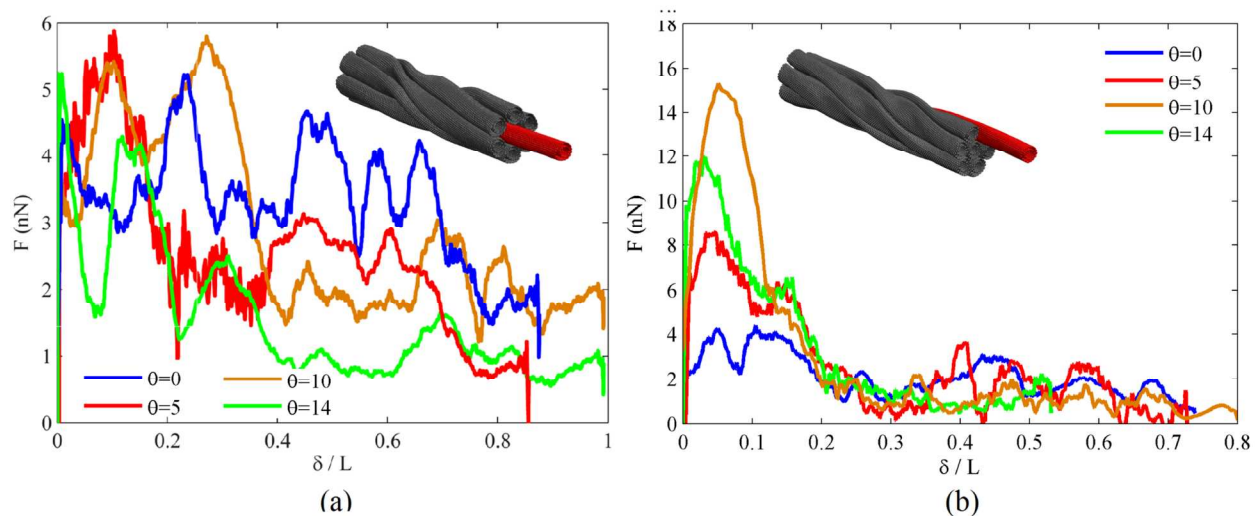


Figure 2: Pull-out forces for the (a) center and (b) side tubes in a bundle of double walled CNTs for four representative angles. Insets show the bundle and the pulled out nanotube is colored in red. The maximum force for pulling out the central nanotube is slightly decreased at higher twist angles, while for the side tube the maximum force increases for the small twist angles and then sharply decreases for the larger twist angles. The maximum pull-out force as a function of twist angle is further studied in Figure 3.

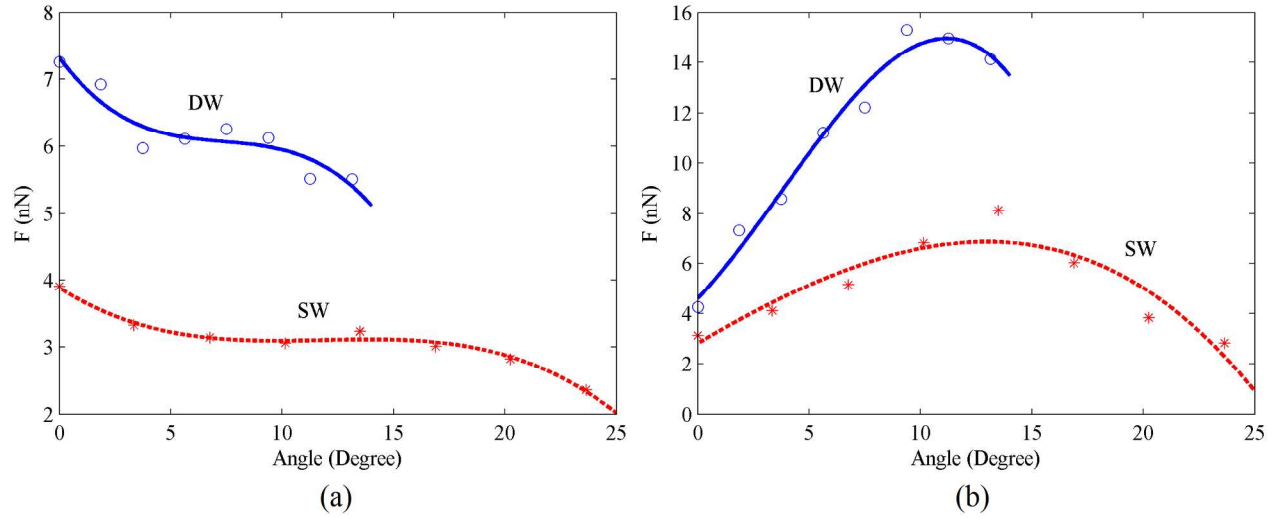


Figure 3: Maximum pullout forces for the (a) middle and (b) side tube in a closed pack bundle as functions of twist angles for both the single and double walled CNTs. The individual data points correspond to full atomistic simulations and the lines are polynomial curves fitted to the data points. The maximum pull-out force for the central nanotube is slightly decreased by increasing the twist angles (a). For the side tube, the maximum pull-out force increases for small twist angles and then decreases for the larger twist angles (b).

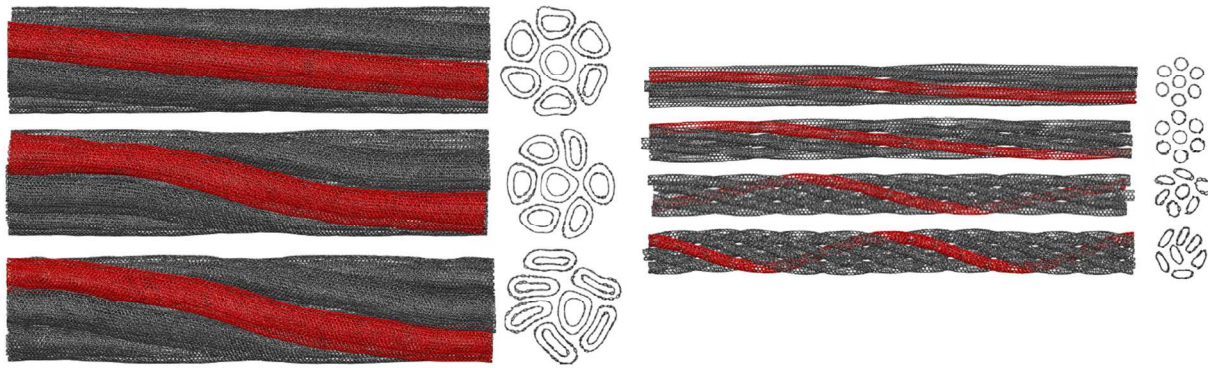


Figure 4: The overall deformed shape of the closed pack bundle and the cross section deformations (at a mid-length section) for both the double walled (left) and single walled (right) nanotube bundles. Twisting makes a distortion in the cross section which increases the contact area between the adjacent tubes and decreases the tubes center lines distances. Further twisting the bundle (last row in each figure) causes excessive deformation in the cross section of individual CNTs in the bundle which weakens the intertube interactions.

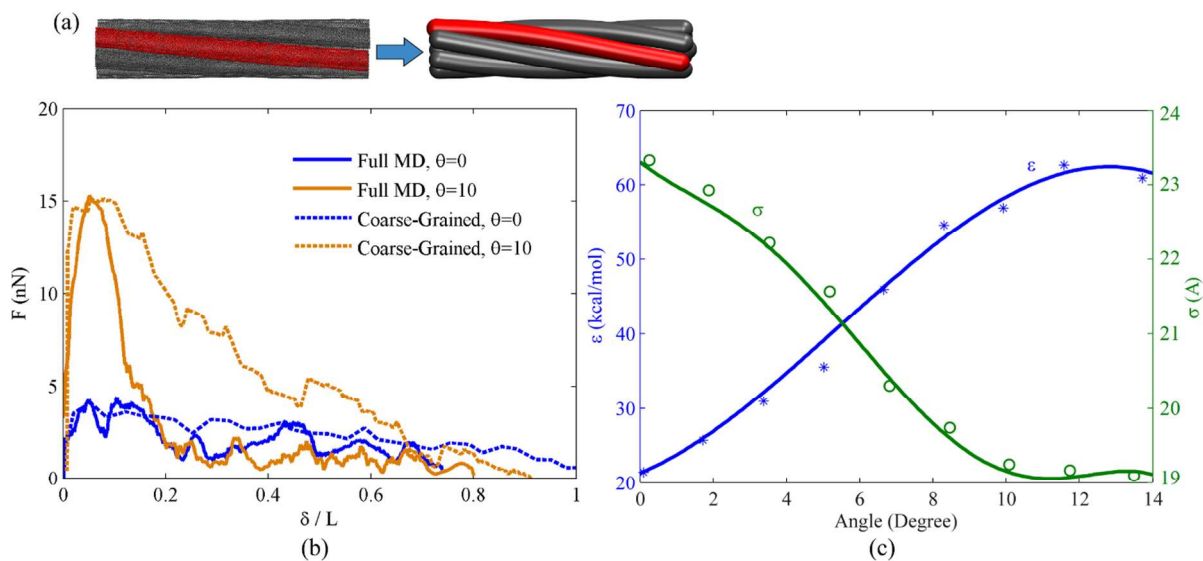


Figure 5: (a) A set of seven closed pack DWNTs modeled by the coarse grained model. (b) A sample of matched force-displacement responses for two different twisting angles and (c) the required updated vdW parameters for achieving the best match between the coarse grained and full atomistic models as functions of twisting angle. The cross section distortions shown in Figure 3 cause an increase in the inter-tube vdW interaction and decreases in the tubes center lines distances (c).

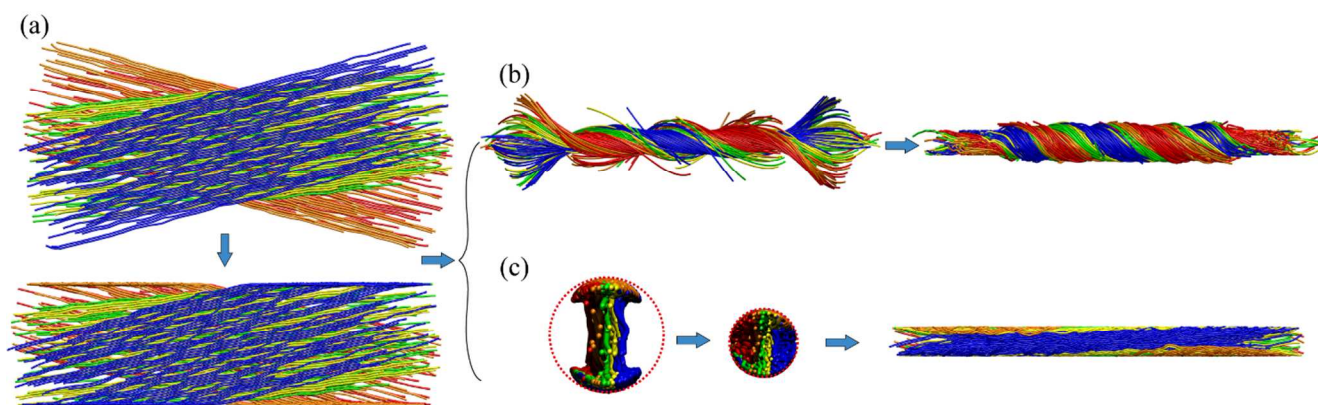


Figure 6: (a) A schematic of the mesoscopic film composed of five CNT layers with random orientations wobbled around the axis. Each layer contains several CNTs with a random length in the range of 50 to 80% the total length of the mat. The initial system is used for constructing (b) twisted and (c) untwisted yarns. Different colors are used for distinguishing the layers.

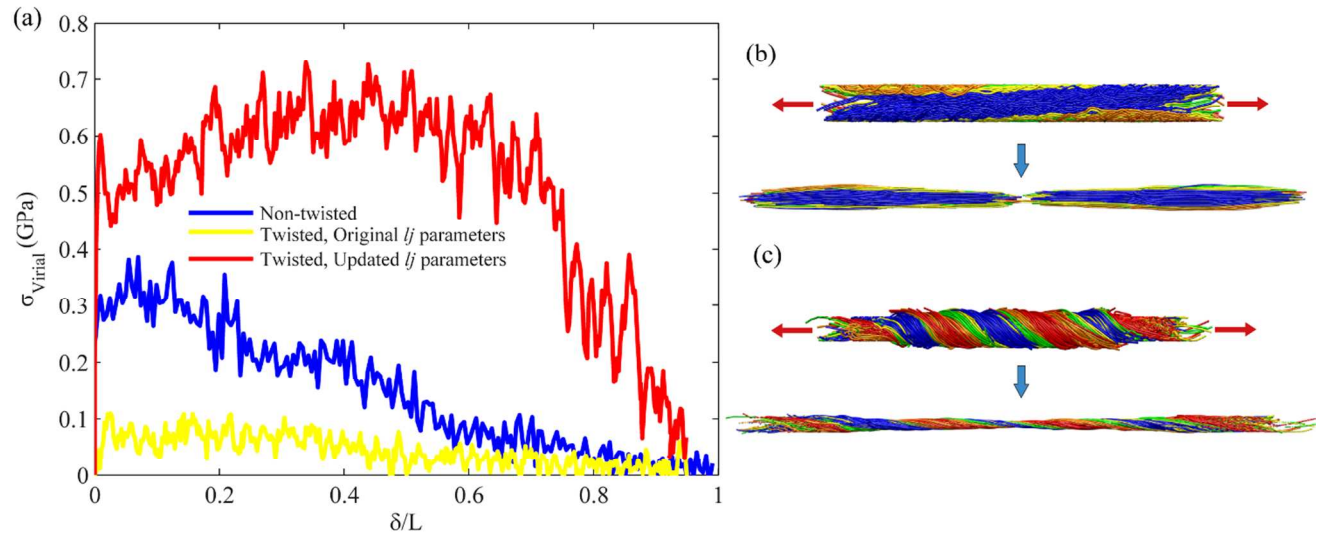


Figure 7: The effect of twisting on the strength of yarns. (a) The stress versus engineering strain for a twisted and untwisted yarn. The stress-strain response predicted by the original coarse grained model is also shown for comparison purposes. (b, c) The deformation of both untwisted and twisted yarns subjected to the axial tension. When the vdW parameters are not updated in the coarse grained model, the simulation predicts a remarkable decrease in the strength by twisting the yarns, which is erroneous. However, the updated coarse grained model, which incorporates the smaller scale deformations by updating the vdW interactions, shows the improvement caused by twisting on both the strength and toughness of the yarn consistent with the experimental results (a). All the stress-strain responses exhibit a sharp initial slope, which is remarkably higher for the twisted yarn. This sharp initial response corresponds to the case that the applied force, which is monotonically increasing, is not enough to overcome the vdW interaction between the tubes and the displacements are negligible. The value of force at which sliding begins is larger for the twisted yarns, mainly because the vdW interactions are stronger.

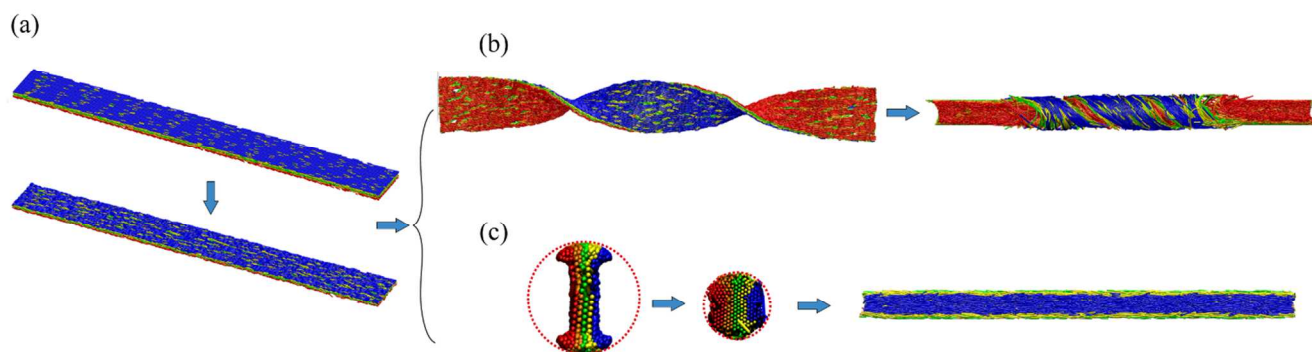


Figure 8: (a) A schematic of the mesoscopic mat composed of five CNT layers with random orientations around the axis. Each layer contains several CNTs with a random length in the range of 5 to 10% the total length of the mat. The initial system is used for constructing (b) twisted and (c) untwisted yarns. Different colors are used for distinguishing the layers.

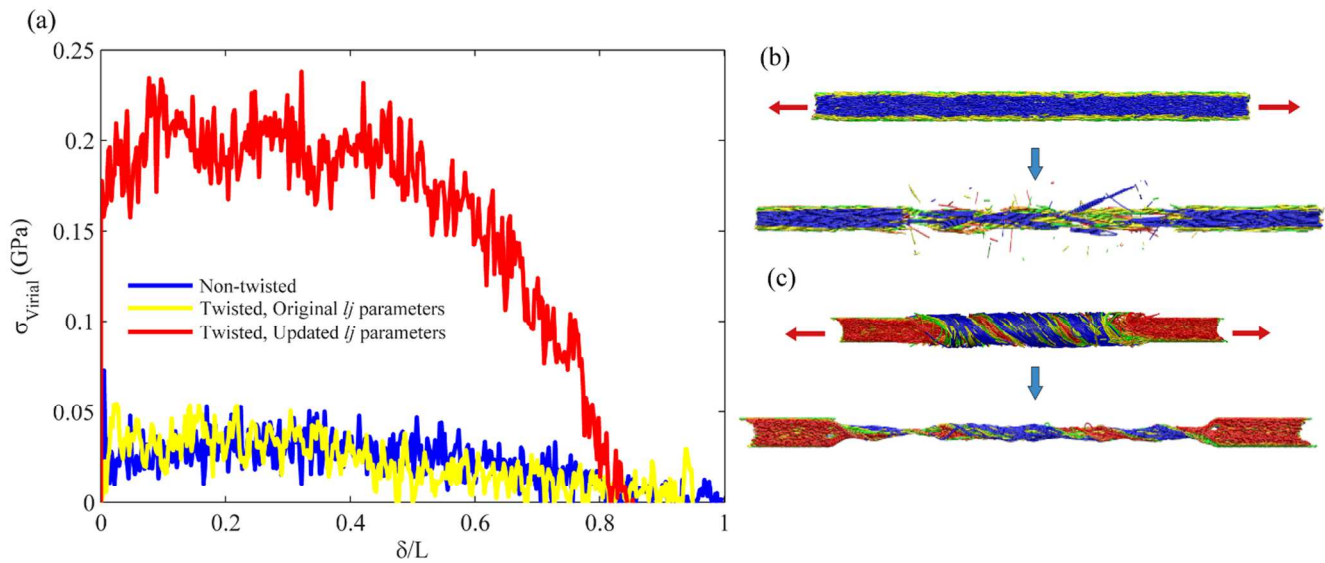


Figure 9: The effect of twisting on the strength of yarns created from spinning and squeezing CNT mats. (a) The stress versus engineering strain for a twisted and untwisted yarn. The stress-strain response predicted by the original coarse grained model is also shown for comparison purposes. (b, c) The deformation of both untwisted and twisted yarns subjected to the axial tension. By using the original vdW parameters the coarse grained model predicts no significant change in the strength by twisting the yarns but the updated coarse grained model shows the improvement caused by twisting on both the strength and toughness of the yarn consistent with the experimental results (a). The stress-strain responses in all the three cases exhibit a sharp initial slope, which is remarkably higher for the twisted yarn. This sharp initial response corresponds to the case that the monotonically increasing force is not enough to overcome the vdW interaction between the tubes and the displacements are negligible. The value of force at which sliding begins is larger for the twisted yarns because the vdW interactions are stronger.